First-in-patient study of OTL78 for intraoperative fluorescence imaging of prostate-specific membrane antigen-positive prostate cancer: a single-arm, phase 2a, feasibility trial

Judith A Stibbe*, Hilda A de Barros*, Daan G J Linders, Shadhvi S Bhairosingh, Elise M Bekers, Pim J van Leeuwen, Philip S Low, Sumith A Kularatne, Alexander L Vahrmeijer, Jacobus Burggraaf†, Henk G van der Poel†

Summary

Background Targeted real-time imaging during robot-assisted radical prostatectomy provides information on the localisation and extent of prostate cancer. We assessed the safety and feasibility of the prostate-specific membrane antigen (PSMA)-targeted fluorescent tracer OTL78 in patients with prostate cancer.

Methods In this single-arm, phase 2a, feasibility trial with an adaptive design was carried out in The Netherlands Cancer Institute, Netherlands. Male patients aged 18 years or older, with PSMA PET-avid prostate cancer with an International Society of Urological Pathology (ISUP) grade group of 2 or more, who were scheduled to undergo robot-assisted radical prostatectomy with or without extended pelvic lymph node dissection were eligible. All patients had a robot-assisted radical prostatectomy using OTL78. Based on timing and dose, patients received a single intravenous infusion of OTL78 (0·06 mg/kg 1–2 h before surgery [dose cohort 1], 0·03 mg/kg 1–2 h before surgery [dose cohort 2], or 0·03 mg/kg 24 h before surgery [dose cohort 3]). The primary outcomes, assessed in all enrolled patients, were safety and pharmacokinetics of OTL78. This study is completed and is registered in the European Trial Database, 2019-002393-31, and the International Clinical Trials Registry Platform, NL8552, and is completed.

Findings Between June 29, 2020, and April 1, 2021, 19 patients were screened for eligibility, 18 of whom were enrolled. The median age was 69 years (IQR 64–70) and median prostate-specific antigen concentration was 15 ng/mL (IQR 9·3–22·0). In 16 (89%) of 18 patients, robot-assisted radical prostatectomy was accompanied by an extended pelvic lymph node dissection. Three serious adverse events occurred in one (6%) patient: an infected lymphocele, a urosepsis, and an intraperitoneal haemorrhage. These adverse events were considered unrelated to the administration of OTL78 or intraoperative fluorescence imaging. No patient died, required a dose reduction, or required discontinuation due to drug-related toxicity. The dose-normalised maximum serum concentration (C_{max}/dose) in patients was 84·1 ng/mL/mg for the 0·03 mg/kg dose and 79·6 ng/mL/mg for the 0·06 mg/kg dose, the half-life was 5·1 h for the 0·03 mg/kg dose and 4·7 h for the 0·06 mg/kg dose, the volume of distribution was 22·9 L for the 0·03 mg/kg dose and 19·5 L for the 0·06 mg/kg dose, and the clearance was 3·1 L/h for the 0·03 mg/kg dose and 3·0 L/h for the 0·06 mg/kg dose.

Interpretation This first-in-patient study showed that OTL78 was well tolerated and had the potential to improve prostate cancer detection. Optimal dosing was 0·03 mg/kg, 24 h preoperatively. PSMA-directed fluorescence imaging allowed real-time identification of visually occult prostate cancer and might help to achieve complete oncological resections.

Funding On Target Laboratories.

Introduction

Prostate cancer surgery is often a compromise between a complete oncological resection and the preservation of vital structures. Developments in preoperative imaging techniques have substantially improved the diagnostic accuracy of prostate cancer detection.[1] Tumour-positive resection margin rates after radical prostatectomy are 6–50% and are correlated with biochemical failure (prostate-specific antigen [PSA] ≥0·2 ng/mL).[2–5] Accurate real-time identification of prostate cancer during surgery might help to achieve complete oncological resections and prevent damage to vital structures.

Fluorescence-guided surgery using tumour-specific tracers is a promising technique to highlight cancer cells and enable real-time surgical guidance.[6–8] For prostate cancer imaging, prostate-specific membrane antigen (PSMA), a transmembrane glycoprotein, is a suitable target because it is overexpressed by 100–1000 times on prostate cancer cells, which is maintained in

Department of Surgery, Leiden University Medical Center, Leiden University, Leiden, Netherlands (J A Stibbe MD, D G J Linders MD, S S Bhairosingh BSc, A L Vahrmeijer MD, Prof J Burggraaf MD); **Department of Urology** (H A de Barros MD, P J van Leeuwen MD, Prof H G van der Poel MD) **and Department of Pathology** (E M Bekers MD), **The Netherlands Cancer Institute, Antoni van Leeuwenhoek Hospital, Amsterdam, Netherlands; On Target Laboratories, West Lafayette, IN, USA** (Prof P S Low PhD, S A Kularatne PhD); **Centre for Human Drug Research, Leiden, Netherlands** (Prof J Burggraaf); **Department of Urology, Amsterdam University Medical Center, Amsterdam, Netherlands** (Prof H G van der Poel)

Correspondence to: Prof Henk G van der Poel, Department of Urology, The Netherlands Cancer Institute, Antoni van Leeuwenhoek Hospital, Amsterdam 1066 CX, Netherlands h.vd.poel@nki.nl

Research in context

Evidence before this study

We searched PubMed on March 15, 2019, for publications in English using the terms "prostate cancer" OR "prostate carcinoma" AND "fluorescence" OR "image guided" AND "surgery" OR "prostatectomy" AND "PSMA". Preclinical experiments and clinical studies have reported that prostate-specific membrane antigen (PSMA) is a suitable target for the imaging and treatment of prostate cancer. This is underlined by studies (including a randomised trial comparing the accuracy of PSMA PET–CT with bone scan and CT scan) that established that PSMA-targeted PET–CT is the most sensitive imaging method for detection of (nodal) metastases of PSMA-positive prostate cancer. However, no peer-reviewed publications of clinical studies describing real-time fluorescence-guided prostatectomy with a PSMA-targeting tracer were identified. The PSMA-targeting near-infrared imaging agent OTL78 has been shown to have a good safety profile in preclinical studies. Visualisation of prostate cancer by fluorescent contrast enhancement in animal models was possible within 2 h after injection with OTL78. The existing evidence shows promising preclinical

results in prostate cancer imaging, but no publications of patient studies exist.

Added value of this study

This study shows that fluorescence-guided prostatectomy (whether or not combined with pelvic lymph node dissection) with OTL78 is safe for use in patients and allows intraoperative, real-time identification of prostate cancer. Additionally, to the best of our knowledge, it is the first clinical trial to show that real-time identification of positive surgical margins and nodal metastases is possible with PSMA-targeted fluorescence imaging.

Implications of all the available evidence

Previous studies established PSMA to be a suitable target in prostate cancer imaging and treatment. Our data show that fluorescence-guided prostatectomy with the PSMA-targeting near-infrared agent OTL78 is safe and feasible and provides accurate intraoperative identification of prostate cancer in real-time. This technique could aid in reducing tumour-positive resection margins and identifying occult nodal metastases, thus improving oncological and functional outcomes in patients with prostate cancer.

metastases.[9,10] PSMA is already used as a target for both PET imaging and treatment in patients with prostate cancer.[11,12] The imaging agent OTL78 consists of a high-affinity PSMA-targeting ligand 2-[3-(1,3-dicarboxypropyl)-ureido]pentanedioic acid (DUPA) conjugated to the near-infrared dye S0456 using a 14-atom-long polyethylene glycol-dipeptide linker. Preclinical data showed that OTL78 allows tumour visualisation with adequate contrast to adjacent healthy tissue and facilitates the assessment of tumour resection margins within 1–2 h after injection.[13] OTL78 was shown to have a good safety profile in healthy human participants (unpublished). There were no safety signals and only two minor adverse events after administration of doses of 0·03 mg/kg and 0·06 mg/kg in healthy volunteers. Both events were mild, resolved without sequelae, and considered unrelated to OTL78.

We aimed to determine the safety, optimal dose, dosing interval, sensitivity, specificity, false-negative rate, and false-positive rate of OTL78 for fluorescence-guided surgery in patients with prostate cancer.

Methods

Study design and participants

This single-arm, phase 2a, feasibility study with an adaptive design was carried out in The Netherlands Cancer Institute, Netherlands. The trial protocol is available in the appendix.

Male patients aged 18 years or older, with PSMA PET-avid prostate cancer with an International Society of Urological Pathology (ISUP) grade group of 2 or more, who were scheduled to undergo robot-assisted radical

prostatectomy with or without extended pelvic lymph node dissection at the NCI were eligible. Patients needed to be clinically fit for surgery and able and willing to comply with study procedures (full eligibility criteria are shown in appendix p 2). The study was conducted in accordance with the Declaration of Helsinki and was approved by the ethics committee at the Leiden University Medical Center, Leiden, Netherlands, and the board of directors of the Netherlands Cancer Institute, Amsterdam, Netherlands. All patients provided written informed consent.

Procedures

OTL78 (On Target Laboratories, West Lafayette, IN, USA) was synthesised under Good Manufacturing Practice through a five-step process by Patheon (part of Thermo Fisher Scientific, Greenville, NC, USA; appendix p 2). All patients received a single dose of OTL78 intravenously over 1 h (appendix p 2). The selected doses were based on animal toxicology that indicated sufficient safety margins in humans; 0·03 mg/kg at 100 times the safety margin and 0·06 mg/kg at 50 times the safety margin. Experiments in mice showed that a 1 h dose interval was sufficient for clear tumour fluorescence after a single dose of 10 nmol/L in 100 μL saline; after 48 h, 50% of fluorescence remained in the tumour.[13] The 1–2 h dose interval in this study was the shortest that could be implemented in the clinical workflow and the 24 h dose interval was chosen to allow decrease in non-specific fluorescence.[13] On the basis of dose and dose interval considerations, three dose cohorts were studied: 0·06 mg/kg OTL78 administered 1–2 h preoperatively

(dose cohort 1); 0·03 mg/kg OTL78 administered 1–2 h preoperatively (dose cohort 2); and 0·03 mg/kg OTL78 administered 24 h preoperatively (dose cohort 3). High fluorescent background signals guided dose reduction and dose interval prolongation. The first evaluation occurred after analysing imaging and safety results from the first three participants. The exact timing of dose interval prolongation was not prespecified and was based on imaging results. Safety was assessed by measuring vital signs, physical examination, electrocardiogram, and clinical laboratory values on the day of infusion and one day after. Adverse events were collected up to 2 weeks after discharge and classified using the National Cancer Institute Common Terminology Criteria for Adverse Events (version 5.0). Blood samples for pharmacokinetic analysis were taken for up to 24 h.

Robot-assisted radical prostatectomies and concomitant extended pelvic lymph node dissections were done using the Da Vinci Si or Xi Surgical System (Intuitive, Sunnyvale, CA, USA) by two experienced urologists (PJvL and HGvdP). The VisionSense near-infrared imaging system (Medtronic, Minneapolis, MN, USA) was used for laparoscopic near-infrared fluorescence imaging through a para-umbilical 12 mm assistant port. The TilePro function of the Da Vinci Surgical System was used to present real-time fluorescence images. Intraoperative near-infrared fluorescence imaging was done before, during, and after resection of prostate and lymph node clusters (defined as the fatty tissue lump dissected from a lymph node region). The peroperative imaging workflow is shown in the appendix (p 3).

Ex-vivo fluorescence imaging of all resected specimens was done on the backtable (ie, a table in the operating theatre equipped for fluorescence imaging of resected specimens) with the VisionSense near-infrared imaging open system. Formalin-fixed prostate and lymph node specimens sectioned to 3–5 mm tissue slices were imaged subsequently (appendix p 3).

Formalin-fixed, paraffin-embedded, and sectioned specimens were evaluated for tumour presence according to ISUP protocols by a board-certified uropathologist (EMB) after haematoxylin and eosin staining (appendix p 4).[14] Microscopic slides were requested from tumour-positive or fluorescent prostate or node regions. Being masked for fluorescence, the uropathologist delineated tumour-positive regions on requested microscopic slides, which were subsequently assessed for tumour volume, ISUP grade group, and extracapsular extension. Tumour volume was stratified into smaller than 0·5 cm³ and 0·5 cm³ or larger, the latter being defined as clinically significant prostate cancer (appendix p 4).[15]

Immunohistochemistry for PSMA evaluation was done on a sequential slide of fluorescent or tumour-positive prostate regions and lymph nodes. The study uro-pathologist scored PSMA expression using the total immunostaining score (appendix p 4).[16] Fluorescence microscopy (near-infrared fluorescence-sensitive Odyssey CLx Imaging system; LI-COR, Lincoln, NE, USA) was done on one formalin-fixed, paraffin-embedded slice to evaluate the correlation between OTL78 fluorescence with tumour presence and PSMA expression (appendix p 4).

Analyses of in-vivo and ex-vivo near-infrared images was done using ImageJ software (version 1.53h, National Institutes of Health, Bethesda, MD, USA). First, images were linearised on the VisionSense player. Signal-to-background ratios were calculated by dividing mean fluorescence intensity—the fluorescence signal divided by the number of pixels—of a fluorescent region by that of the adjacent background area. Signal-to-background ratio was preferred over tumour-to-background ratio considering the presence of PSMA expression in normal tissue. A signal-to-background ratio of 1·5 or more was considered sufficient to discriminate lesions from background.[17] Pathology results were used as gold standard for tumour detection in all analyses. The signal-to-background ratio was arbitrarily set to 1 when no discrimination between a target lesion and background was possible. For in-vivo and ex-vivo (backtable) fluor-escence analysis, the prostate was divided into nine regions modified from the Ginsburg protocol (appendix p 5).[18,19] In-vivo and ex-vivo (backtable) fluorescence analysis of lymph nodes was done at cluster level and also on an individual lymph node basis ex vivo (appendix p 3).

In the near-infrared fluorescence images of the resection bed, signal-to-background ratio was defined as the mean fluorescence intensity of the residual fluorescent tissue in the resection bed divided by the mean fluorescence intensity of adjacent tissue.

Patient race was self-reported.

Outcomes

The primary outcomes were the safety and pharmaco-kinetics of OTL78. Safety included treatment-emergent adverse events, serious treatment-emergent adverse events, abnormal clinical laboratory tests, abnormal vital signs, abnormal clinical examination, including assessment of injection site, abnormal 12-lead ECG, study drug withdrawal due to treatment-emergent adverse events, and treatment administered for treatment-emergent adverse events. Pharmacokinetics included the area under the serum concentration-time curve from zero to infinity (AUC_{0-inf}), the maximum serum concentration (C_{max}), the area under the serum concentration-time curve from zero to t of the last measured concentration above the limit of quantifi-cation (AUC_{0-last}), the time to reach maximum plasma concentration (t_{max}), and the terminal disposition rate constant (λz) with the respective half-life ($t\frac{1}{2}$). Not all parameters are reported. For instance, AUCs are not reported because these were used to calculate the primary pharmacokinetic parameters such as clearance and volume of distribution. Similarly, we have not reported the terminal rate constant, but the more informative elimination half-life.

Secondary outcomes were sensitivity, defined as the true-positive rate (true positives / [true positives + false negatives]) of OTL78 for detection of prostate cancer with histopathology as reference; specificity, defined as the true-negative rate (true negatives / [true negatives + false positives]) of OTL78 for detection of prostate cancer with histopathology as reference; the false-negative rate (false negatives / [false negatives + true positives]) of OTL78 for detection of prostate cancer with histopathology as reference; the false-positive rate (false positives / [false positives + true negatives]) of OTL78 for detection of prostate cancer with histopathology as reference; and determination of the optimal dose and dose interval of OTL78 for real-time identification of prostate cancer as measured by the signal-to-background ratio.

The exploratory outcome was to evaluate the surgeons' rating for the utility of OTL78 intravenous injection and imaging system in visualising prostate cancer and lymph nodes during surgery.

Statistical analysis

The sample size of 18 patients was chosen on the basis of practical and clinical considerations.[20–22] Primary, secondary, and exploratory outcomes were assessed in all patients. Subgroup analyses of signal-to-background ratios by tumour grade, tumour volume, and PSMA expression were done post-hoc. Descriptive statistics are presented as frequencies with percentages (eg, for adverse events) or medians and IQRs (eg, for signal-to-background ratios). To account for within-subject correlation in sensitivity and specificity calculations, we used logistic regression models with cluster-robust standard errors, with clustering at patient level. The Wilson method was used to calculate 95% CIs when sensitivity or specificity in subgroup analyses was 100% or when analyses were based on a single patient. To determine the optimal dose and dose interval of OTL78, differences in signal-to-background ratios between dose cohorts were assessed using linear regression analyses on log-transformed signal-to-background ratios. Differences in signal-to-background ratios between dose cohorts, tumour grades, tumour volumes, and PSMA expression levels were assessed with linear regression analyses on log-transformed signal-to-background ratios. Statistical significance was determined by two-tailed t tests based on cluster-robust standard errors. Cluster-robust 95% CI calculations, t tests and p value analyses were done post hoc. Statistical tests were done using R version 4.0.1. A p value less than 0·050 was considered statistically significant. Data are summarised in box-and-whisker plots generated in GraphPad Prism 9 (GraphPad Software, La Jolla, CA, USA). Non-compartmental analysis on the pharmacokinetic data was performed using R-software (version 4.0.3) with the PKNCA package (version 0.9.5) The study is registered in the European Trial Database, 2019-002393-31, and the International Clinical Trials Registry Platform, NL8552.

Role of the funding source

The funder of the study had no role in data collection, data analysis, data interpretation, or writing of the report. The study was designed and protocol written by the study team at the Centre for Human Drug Research, with final approval from the funder. The manuscript was shared with the sponsor for review.

Results

Between June 29, 2020, and April 1, 2021, 19 patients with biopsy-confirmed prostate cancer were screened for enrolment. 18 patients were included; one patient was ineligible for participation because of an intercurrent event between consent and surgery. Median age at prostate cancer diagnosis was 69 years (IQR 64–70), and median initial PSA was 15 ng/mL (IQR 9·3–22·0; table 1). 12 (67%) of 18 patients had prostate cancer with ISUP grade group 3 or more. Median interval between PSMA–PET imaging and robot-assisted radical prostatectomy was 33 days (IQR 27–42; full data for the interval between PSMA–PET imaging and surgery not shown). All patients had a robot-assisted radical prostatectomy, and 16 (89%) of 18 patients also had an extended pelvic lymph node dissection due to the estimated risk of nodal metastases.

No clinically meaningful changes in vital signs, laboratory parameters, or electrocardiograms were observed. 42 adverse events were observed (appendix pp 6–7), of which 37 had an incidence of 10% or more (table 2). Three serious adverse events were observed in one (6%) patient (infected lymphocele drained percutaneously, urosepsis treated with antibiotics and fluid resuscitation, and an intraperitoneal haemorrhage requiring percutaneous drainage). All adverse events and serious adverse events were considered unrelated to OTL78 administration or fluorescence imaging. No patient died, required dose reduction, or required discontinuation due to drug-related toxicity.

The dose-normalised maximum serum concentration (C_{max}/dose) in patients was 84·1 ng/mL/mg for the 0·03 mg/kg dose and 79·6 ng/mL/mg for the 0·06 mg/kg dose, the half-life was 5·1 h for the 0·03 mg/kg dose and 4·7 h for the 0·06 mg/kg dose, the volume of distribution was 22·9 L for the 0·03 mg/kg dose and 19·5 L for the 0·06 mg/kg dose, and the clearance was 3·1 L/h for the 0·03 mg/kg dose and 3·0 L/h for the 0·06 mg/kg dose.

The first three patients (dose cohort 1) received 0·06 mg/kg OTL78 1–2 h before surgery. Because of high background uptake in healthy prostate tissue and benign lymph nodes, and non-specific bladder neck fluorescence due to leakage of OTL78-containing urine after bladder incision, the next 11 patients (dose cohort 2) received 0·03 mg/kg 1–2 h before surgery. Due to persistent uptake in benign lymph nodes, the last four patients (dose cohort 3) received 0·03 mg/kg 24 h before surgery. The intensity of non-specific bladder neck fluorescence decreased with lower OTL78 dose and longer dose interval (appendix p 5).

	Age at diagnosis, years	Race	Clinical TNM stage	MRI T stage	Prostate-specific antigen at diagnosis, ng/mL	Biopsy ISUP grade group	Pathological TNM stage	Diameter largest lymph node metastasis, mm	Pathological ISUP grade group	Resection margin	Prostate-specific antigen at last follow up
Dose cohort 1: 0·06 mg/kg OTL78 1–2 h preoperatively											
Patient 1	72	White	cT1cN0M0	mT3b	17·0	2	pT3bN0	··	5	R0	<0·01
Patient 2	69	White	cT2N0M0	mT3a	6·6	4	pT3aN0	··	2	R0	<0·01
Patient 3	69	White	cT1cN0M0	mT2	19·0	2	pT3aN0	··	3	R1	<0·01
Dose cohort 2: 0·03 mg/kg OTL78 1–2 h preoperatively											
Patient 4	63	White	cT2N1M0	mT3b	33·0	3	pT3bN1	30·0	3	R1	1·40
Patient 5	67	White	cT1cN0M0	mT3a	18·0	2	pT3aNx	··	3	R0	<0·01
Patient 6	59	White	cT1cN0M0	mT3	16·0	4	pT3aN1	1·8	2	R1	0·01
Patient 7	69	White	cT2N0M0	mT3a	5·7	3	pT3aN0	··	2	R1	<0·01
Patient 8	70	White	cT1cN0M0	mT2	9·3	3	pT3aNx	··	2	R0	<0·01
Patient 9	48	White	cT1cN0M0	mT2	9·4	3	pT3bN1	2·0	2	R0	0·24
Patient 10	67	White	cT2N0M0	mT2	23·0	4	pT2N0	··	2	R1	0·17
Patient 11	63	White	cT2N0M0	mT3a	37·4	2	pT3aN0	··	3	R1	0·03
Patient 12	73	White	cT1cN1M0	mT2a	11·0	2	pT3aN0	··	3	R0	<0·01
Patient 13	68	White	cT3aN0M0	mT2	6·3	4	pT2N0	··	2	R0	<0·01
Patient 14	69	White	cT2aN0M0	mT3a	13·1	3	pT3aN1	3·6	3	R0	0·02
Dose cohort 3: 0·03 mg/kg OTL78 24 h preoperatively											
Patient 15	72	White	cT1cN0M0	mT3b	26·0	5	pT3bN1	2·6	5	R0	0·01
Patient 16	60	White	cT1cN0M0	mT3b	29·2	3	pT3bN0	··	5	R0	0·05
Patient 17	69	White	cT2N0M0	mT3b	7·1	2	pT3bN0	··	3	R1	<0·01
Patient 18	73	White	cT1cN0M0	mT2	14·0	3	pT3aN0	··	3	R1	0·12

ISUP=International Society of Urological Pathology.

Table 1: Demographics and tumour characteristics of patients who had fluorescence-guided surgery using OTL78

154 prostate regions were imaged in vivo, of which 65 (42%) contained prostate cancer (figure 1A–C, appendix pp 8–9). Due to technical limitations, in-vivo imaging with the VisionSense imaging system was not possible in one patient. The in-vivo sensitivity and specificity for prostate cancer detection with OTL78 in dose cohorts 1, 2 and 3 are shown in the appendix (pp 8–9). False-positive and false-negative rates are shown in the appendix (pp 8–9). With decreasing dose and increasing dose interval, the mean fluorescence intensity of both tumour and benign background decreased (figure 1B), resulting in a median in-vivo signal-to-background ratio of 1·0 (IQR 1·0–1·6) in dose cohort 1, 1·3 (1·0–1·7) in dose cohort 2, and 1·9 (1·0–2·3) in dose cohort 3 (figure 1C).

Ex-vivo backtable imaging showed prostate cancer in 68 (42%) of 163 prostate regions (figure 1D–F, appendix pp 8–9). The sensitivity of OTL78 for prostate cancer detection was higher with ex-vivo (backtable) than in-vivo imaging in all dose cohorts (appendix pp 8–9). Ex-vivo false-positive and false-negative rates are shown in the appendix (pp 8–9). Similar to in-vivo fluorescence imaging results, the highest median ex-vivo signal-to-background ratio was in dose cohort 3 (figure 1F).

	Grade 1–2	Grade 3
Constipation	2 (11%)	0
Lymphocele	0	1 (6%)
Lymphoedema	10 (56%)	0
Haematoma	5 (28%)	0
Haematuria	4 (22%)	0
Haemorrhage	0	1 (6%)
Myalgia	3 (17%)	0
Urinary incontinence	5 (28%)	0
Urinary tract infection	3 (17%)	0
Urosepsis	0	1 (6%)
Wound complication	2 (11%)	0

Data are n (%). Grade 1 or 2 adverse events occurring in 10% or more of patients per dose cohort and all adverse events of grade 3 or higher are reported. No grade 4–5 adverse events occurred. Grading according to Common Terminology Criteria for Adverse Events (version 5.0).

Table 2: Adverse events by highest grade per patient (n=18)

At histopathological examination, 272 tumour areas were identified on haematoxylin and eosin-stained prostate slides (table 3). Near-infrared fluorescence
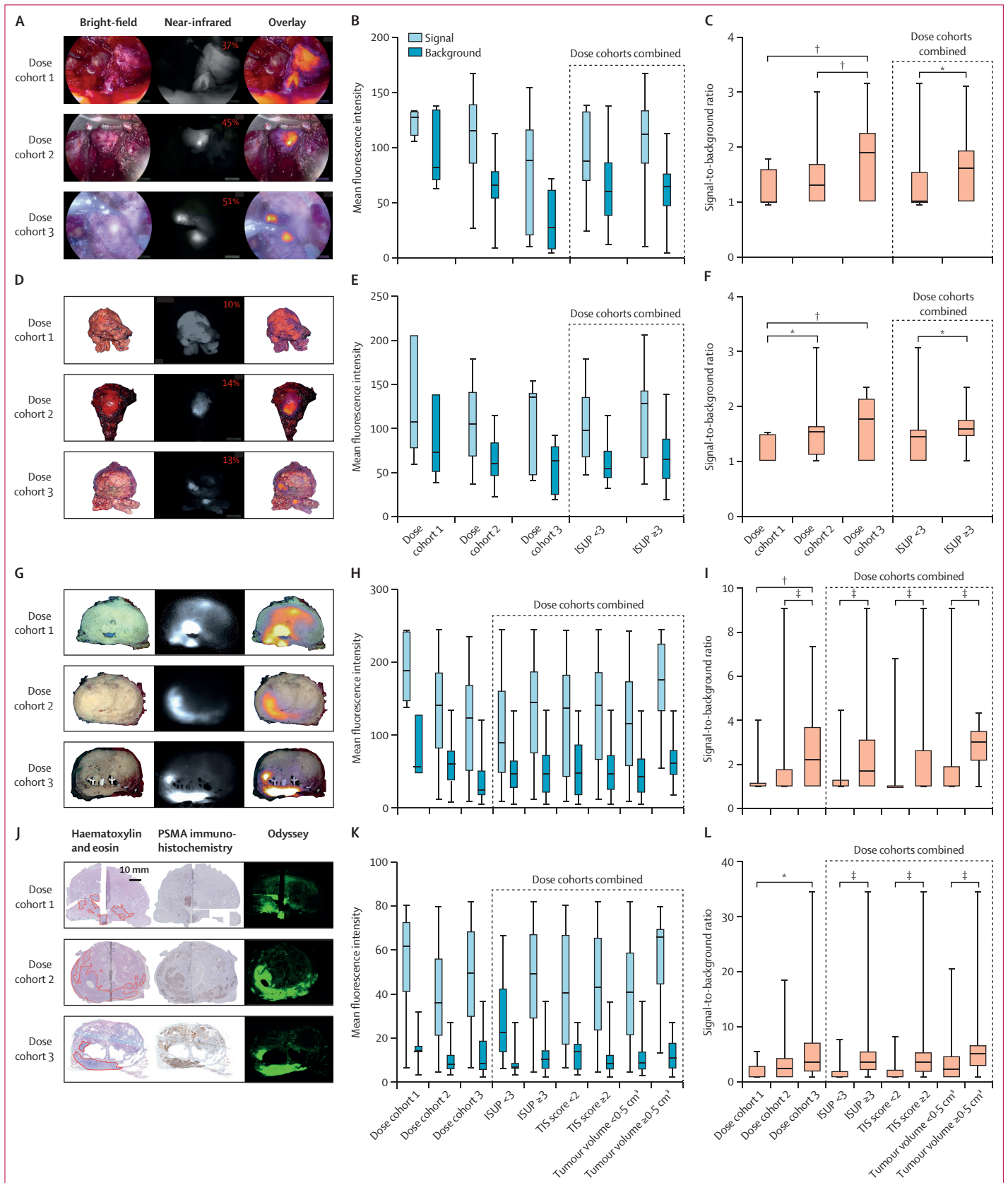
Figure 1: Fluorescence-guided surgery using OTL78
(A) In-vivo bright-field, near-infrared greyscale, and fluorescence colour overlay prostate imaging of patients in dose cohorts 1, 2, and 3 using the Visionsense near-infrared imaging system for laparoscopic fluorescence imaging. (B) In-vivo mean fluorescence intensity of tumour and background according to the dose cohort and the ISUP grade. (C) In-vivo signal-to-background ratio. (D) Ex-vivo bright-field, near-infrared greyscale, and fluorescence colour overlay prostate imaging of patients in dose cohorts 1, 2, and 3. Note a high level of false-positive fluorescence uptake in the entire prostate in dose cohort 1. (E) Ex-vivo mean fluorescence intensity of tumour and background according to the dose cohort and the ISUP grade. (F) Ex-vivo signal-to-background ratio. (G) Histopathological evaluation of sectioned specimens using the Visionsense near-infrared imaging open-system. (H) Mean fluorescence intensities for gross macroscopy. (I) Signal-to-background ratios for gross macroscopy. (J) Microscopy slides corresponding to images in G imaged with the Odyssey CLx Imaging system. (K) Mean fluorescence intensities for microscopy. (L) Signal-to-background ratios for microscopy. Box-and-whisker plots show the minimum, first quartile, second quartile, third quartile, and maximum signal-to-background ratio. ISUP=International Society of Urological Pathology. PSMA=prostate-specific membrane antigen. TIS=total immunostaining score. *p<0·050. †p<0·010. ‡p<0·0010.

imaging of corresponding gross macroscopic prostate whole mounts using the VisionSense near-infrared imaging system located 110 (40%) of 272 lesions (figure 1G–I, table 3). The sensitivity and false-negative rate of near-infrared fluorescence imaging on gross macroscopic prostate whole mounts was primarily dependent on tumour volume, dose and timing of OTL78, and, to a lesser extent, on ISUP grade and

PSMA expression on immunohistochemistry in post-hoc analyses (table 3). Specificity and false-positive rates were not calculated for histopathology, as only tumour-positive or fluorescent prostate slides were requested and processed for imaging.

In post-hoc analyses, OTL78 allowed visualisation of 194 (71%) of 272 lesions on microscopic prostate slides during fluorescence microscopy (figure 1J–L; table 3). Fluorescence imaging sensitivity and signal-to-background ratio at pathology increased with larger tumour volume, dose interval extension, the 0·03 mg/kg OTL78 dose, higher ISUP grade, and higher immunohistochemical PSMA expression (figure 1L, table 3). In 12 (67%) of 18 patients, OTL78 did not only target PSMA-expressing tumours but, to a lesser extent, 19 benign prostate zones (appendix p 10). PSMA overexpression was present in 17 (90%) of 19 false-positive prostate zones.

The effect of OTL78 dose de-escalation and dose interval prolongation on lymph node detection was evaluated post-hoc in 16 patients who had an extended pelvic lymph node dissection (figure 2). 79 lymph node clusters were removed, seven (9%) of which contained metastases (appendix p 11). In-vivo fluorescence imaging detected four metastatic lymph node clusters (median metastasis size of 1·9 mm [IQR 1·8–2·7]), of which one was detected on preoperative PSMA PET–CT (data not shown). When OTL78 was administered 1–2 h before surgery (dose cohort 1 and dose cohort 2), 13 (22%) of

	Gross macroscopy (VisionSense)					Microscopic slides (Odyssey CLx)				
	Overall	True positive	False negative	Sensitivity (95% CI)	False-negative rate (95% CI)	Overall	True positive	False negative	Sensitivity (95% CI)	False-negative rate (95% CI)
Dose cohort										
1	30	7	23	23·3% (4·3–67·5)	76·7% (32·5–95·7)	30	13	17	43·3% (7·2–88·3)	56·7% (11·8–92·8)
2	167	56	111	33·5% (25·8–42·3)	66·5% (57·7–74·2)	167	119	48	71·3% (54·6–83·6)	28·7% (16·4–45·4)
3	72	47	25	65·3% (53·8–75·2)	34·7% (23·6–44·8)	70	62	8	88·6% (74·9–95·3)	11·4% (4·3–24·1)
Missing	3	··	··	··	··	5	··	··	··	··
ISUP grade group										
1–2	97	24	73	24·7% (14·7–38·5)	75·3% (61·5–85·3)	97	42	55	43·3% (25·8–62·6)	56·7% (37·4–74·2)
≥3	169	86	83	50·9% (36·0–65·6)	49·1% (31·6–65·3)	167	149	18	89·2% (82·3–93·7)	10·8% (6·2–17·2)
Missing	6	··	··	··	··	8	··	··	··	··
Tumour volume										
<0·5 cm³	244	87	157	35·7% (25·5–47·3)	64·3% (52·7–74·5)	242	170	72	70·2% (55·3–81·8)	29·8% (18·2–44·7)
≥0·5 cm³	25	23	2	92·0% (70·8–98·2)	8·0% (1·8–29·2)	25	24	1	96·0% (78·3–99·4)	4·0% (0·6–21·7)
Missing	3	··	··	··	··	5	··	··	··	··
PSMA expression										
Weak	27	3	24	11·1% (2·7–36·2)	88·9% (63·8–97·3)	27	4	23	14·8% (5·1–35·8)	85·2% (64·2–94·9)
Moderate	48	12	36	25·0% (14·7–39·1)	75·0% (60·9–85·3)	48	25	23	52·1% (32·4–71·2)	47·9% (28·8–67·6)
Intense	187	92	95	49·2% (33·8–64·8)	50·8% (35·3–66·2)	185	159	26	85·9% (76·0–92·2)	14·1% (7·8–24·0)
Missing	10	··	··	··	··	12	··	··	··	··

ISUP=International Society of Urological Pathology. PSMA=prostate-specific membrane antigen.

Table 3: Sensitivity of OTL78-based near-infrared fluorescence imaging for prostate cancer detection on gross macroscopy and microscopic slides
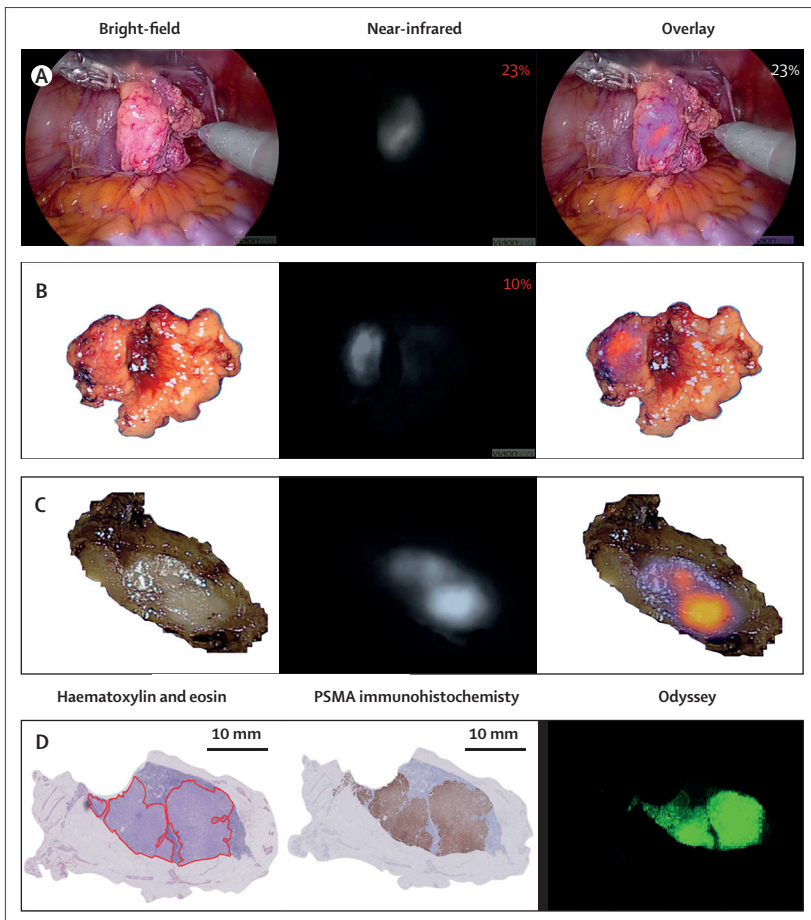
Figure 2: Fluorescence imaging of a lymph node metastasis
(A) In-vivo and (B) ex-vivo (backtable) bright-field, near-infrared and fluorescence color overlay imaging of a lymph node metastasis within a lymph node cluster using the VisionSense imaging system. (C) Fluorescence imaging of the formalin-fixed metastatic lymph node isolated from the lymph node cluster at gross macroscopy. (D) Corresponding haematoxylin and eosin tumour delineation, PSMA immunohistochemistry, and fluorescence imaging show a PSMA-positive metastatic lymph node with OTL78 uptake. PSMA=prostate-specific membrane antigen.

59 lymph node clusters were false-positive in vivo. Five (38%) of these 13 false positives were in dose cohort 1, and eight (62%) were in dose cohort 2 (appendix p 11).

Post-hoc ex-vivo imaging identified four (57%) of seven metastatic lymph node clusters. There were 21 false-positive lymph node clusters, all of which were observed in dose cohort 1 (six [29%]) and dose cohort 2 (15 [71%]; appendix p 11). OTL78 dose de-escalation and interval prolongation led to a lower false-positive lymph node cluster rate and a higher false-negative rate, in vivo and ex vivo (appendix p 11). The false-negative rate and sensitivity in dose cohort 3 were based on a single patient, because only one patient had nodal involvement (appendix pp 11–12).

Post-hoc gross-macroscopic and microscopic fluorescence imaging of individual lymph nodes (n=289) identified all nine metastatic lymph nodes (appendix p 12) with a median signal-to-background ratio of 3·5 (IQR 2·7–5·3) for gross macroscopy and 8·8 (3·1–20·3)

for microscopy (signal-to-background ratio plots of lymph node fluorescence imaging are not shown). Because only tumour-positive or fluorescent microscopic slides were requested and imaged, specificity and false-positive rates were not calculated. Post-hoc immunohistochemistry confirmed PSMA expression in metastatic lymph nodes, and false-positive lymph nodes showed no PSMA expression (immunohistochemistry data of lymph nodes not shown). Only dose cohort 1 and dose cohort 2 showed false-positive lymph nodes on gross-macroscopic and microscopic fluorescence imaging.

Eleven prostatic surgical margins were tumour-positive in post-hoc analysis of histopathology in eight patients (table 1, appendix p 13). All positive margins contained PSMA-expressing prostate cancer cells. Fluorescence signals at the location of the margin were shown in nine (82%) of 11 tumour-positive margins by in-vivo fluorescence imaging and in 11 (100%) by ex-vivo fluorescence imaging (figure 3; appendix p 13). 12 patients had additional resection of residual fluorescent tissue after prostatectomy. In three (25%) of 12 patients this residual fluorescent tissue was due to remnant prostate cancer. In nine (75%) of 12 patients, all of whom received OTL78 on the day of surgery, resection of residual fluorescence tissue did not show tumour (appendix p 13). Another patient showed residual fluorescence in the resection bed that could not be resected because of a high risk of rectal perforation. In the 24 h dose interval, residual fluorescence was observed only in the case of prostate cancer residue.

Discussion

The findings from this first-in-patient study with OTL78 suggest that this PSMA-targeted near-infrared imaging agent is safe and allows real-time in-vivo and ex-vivo imaging of prostate cancer. No adverse events or serious adverse events related to administration of OTL78 or near-infrared fluorescence occurred. Although the overall adverse event rate in our study appears to be higher than in the existing literature, this might be due to the lower quality of complication reporting in the predominantly retrospective literature. The serious adverse event rate of 6% is similar to the 0·6–5·2% in other radical prostatectomy series.[23,24] Furthermore, adverse events observed in this study have been associated with robot-assisted radical prostatectomies and extended pelvic lymph node dissections in numerous series, making an association between surgery and adverse events highly likely.[25]

A single intravenous dose of 0·03 mg/kg OTL78 administered 24 h before surgery provided the highest signal-to-background ratio and the best tumour visual-isation in vivo and ex vivo, with obvious differences between both methods; OTL78 showed high accuracy for prostate cancer detection in the optimal dose and timing regimen. False-negative lesions on fluorescence micros-copy were often characterised by either weak PSMA

expression, low tumour volume, or low ISUP grade.[13] In all dose cohorts, ex-vivo backtable fluorescence analysis showed higher sensitivity for detecting prostate cancer lesions than in vivo. The limited range of motion of the laparoscope, which caused difficulties in the in-vivo visualisation of distal prostate regions deep within the pelvis (eg, apex), might explain this difference, because ex-vivo prostate imaging allowed inspection of the entire prostate surface.

OTL78 allowed in-vivo visualisation of metastatic lymph node clusters. False-positive lymph nodes were observed only when patients received OTL78 on the day of surgery and not in the 24 h dosing interval. Immunohistochemistry showed no PSMA expression in false-positive lymph nodes, suggesting non-specific fluorescence staining occurred relatively shortly after administration. No false-positive lymph node clusters were identified on implementation of the 24 h dose interval, probably due to increased wash-out of OTL78 from the lymphatic system. However, this came with a higher false-negative rate for lymph nodes at in-vivo and ex-vivo backtable imaging. We hypothesise that overlying adipose tissue might limit the detection of fluorescent metastatic nodes due to the limited penetration depth of near-infrared light.[26] This is not the case with fluorescence microscopy, which showed that OTL78 identified each metastatic lymph node, providing evidence of OTL78 accumulation in PSMA-expressing prostate cancer cells within lymph nodes. These results confirm that OTL78 dose and the timing of imaging contribute to the accuracy of lymph node detection. However, these findings should be interpreted cautiously as only a small number of metastatic lymph nodes were found in this study.

The use of OTL78 enabled real-time surgical margin assessment. The higher ex-vivo than in-vivo surgical margin detection rate can be explained by the mid-apical location of two positive surgical margins, which is difficult to reach with the laparoscope. Additionally, assessment of the resection bed allowed the surgeons to detect occult residual fluorescent prostate cancer. Residual prostate cancer could not be confirmed histologically in one patient due to the risk of rectal perforation. However, the intensity and location of the signal corresponded to the positive surgical margin location on the resected prostate, make it plausible that residual fluorescence was remnant prostate cancer. We propose that a combination of ex-vivo fluorescence-guided surgical margin evaluation and in-vivo assess-ment of the resection bed (with particular attention to fluorescent areas on the resected prostate) could provide an efficient, real-time technique to achieve complete surgical resection.

Several limitations of our study need to be addressed. The small sample size limited robust statistical analyses, and several challenges of PSMA-targeted fluorescence imaging were identified. First,
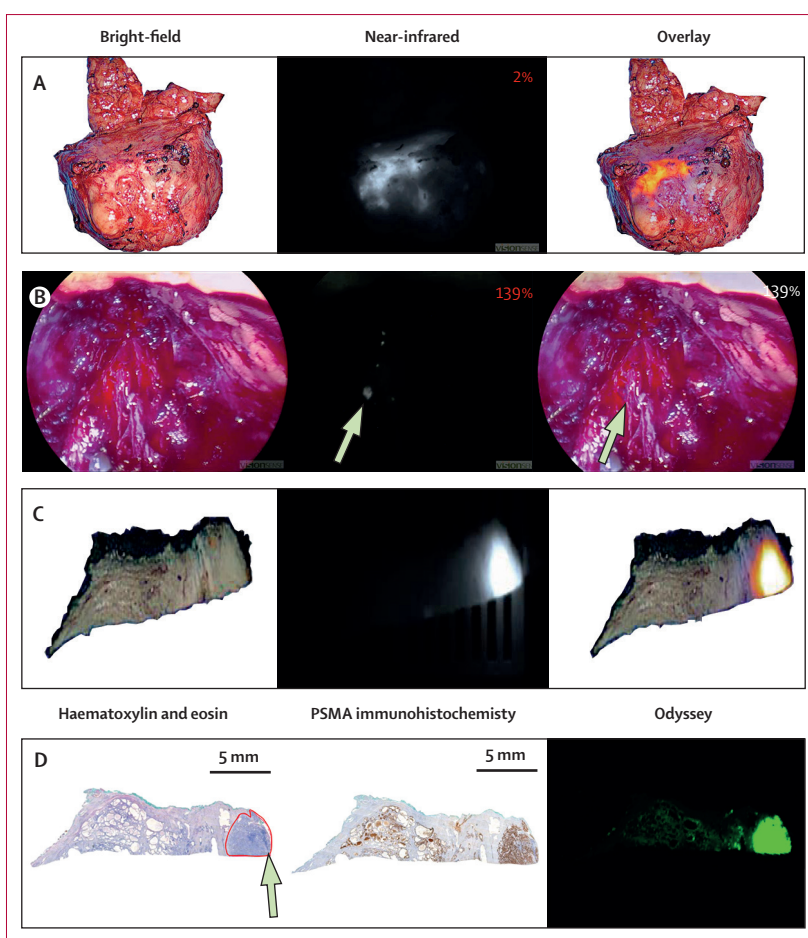
Figure 3: **Fluorescence workflow for surgical margin and resection bed assessment**
(A) The entire prostate is imaged directly after resection ex vivo on the backtable. Increased fluorescence signal is visible at the apex. (B) Subsequent assessment of the resection bed shows residual fluorescence signal (indicated with an arrow) where the apex used to be. (C) A fluorescent, PSMA-expressing positive surgical margin is seen on ex-vivo gross macroscopy. (D) A fluorescent, PSMA-expressing positive surgical margin (indicated with an arrow) is seen on microscopic slide imaging and on histopathology. PSMA=prostate-specific membrane antigen.

fluorescence in benign prostate tissue with PSMA overexpression, particularly the central zone of the prostate, which is known to overexpress PSMA as was the case in our study, made it difficult to distinguish tumour from background in these areas.[27,28] However, prostate cancer in the central zone is rare and most tumours arise from the peripheral zone where PSMA overexpression is uncommon.[29] Second, contamination of the surgical field by renally excreted OTL78 hindered intraoperative assessment of the basal margin of the prostate. Dose interval prolongation allowed more urinary excretion of OTL78 before imaging and consequently less contamination of the surgical field. Third, the laparoscopic camera was positioned by the bedside assistant under verbal guidance of the urological surgeon sitting at the distant surgical console. Finally, in-vivo fluorescence imaging of the apex of the prostate deep in the pelvis was challenging with the laparoscope. Ex-vivo imaging in the surgical

theatre allowed visualisation of the entire prostate and helped overcome this limitation. Integrating fluorescence imaging hardware into robotic surgery systems (eg, FireFly technology [Intuitive Surgical, Sunnyvale, CA, USA]) can improve deep pelvic visualisation and facilitate robot-assisted fluorescence-guided surgery within the surgical workflow.

In summary, our data show the safety and feasibility of OTL78 for PSMA-targeted fluorescence-guided surgery in patients with prostate cancer. OTL78 can intraoperatively enhance visualisation of primary prostate tumours, surgical margins, residual prostate cancer in the resection bed, and nodal metastases. These promising results warrant validation in a larger cohort of patients with primary prostate cancer.

References
1 Hofman MS, Lawrentschuk N, Francis RJ, et al. Prostate-specific membrane antigen PET-CT in patients with high-risk prostate cancer before curative-intent surgery or radiotherapy (proPSMA): a prospective, randomised, multicentre study. *Lancet* 2020; **395:** 1208–16.

2 Martini A, Gandaglia G, Fossati N, et al. Defining clinically meaningful positive surgical margins in patients undergoing radical prostatectomy for localised prostate cancer. *Eur Urol Oncol* 2021; **4:** 42–48.

3 Moris L, Gandaglia G, Vilaseca A, et al. Evaluation of oncological outcomes and data quality in studies assessing nerve-sparing versus non-nerve-sparing radical prostatectomy in nonmetastatic prostate cancer: a systematic review. *Eur Urol Focus* 2022; **8:** 690–700.

4 Stephenson AJ, Kattan MW, Eastham JA, et al. Defining biochemical recurrence of prostate cancer after radical prostatectomy: a proposal for a standardized definition. *J Clin Oncol* 2006; **24:** 3973–78.

5 Yossepowitch O, Bjartell A, Eastham JA, et al. Positive surgical margins in radical prostatectomy: outlining the problem and its long-term consequences. *Eur Urol* 2009; **55:** 87–99.

6 Hernot S, van Manen L, Debie P, Mieog JSD, Vahrmeijer AL. Latest developments in molecular tracers for fluorescence image-guided cancer surgery. *Lancet Oncol* 2019; **20:** e354–67.

7 Stummer W, Pichlmeier U, Meinel T, Wiestler OD, Zanella F, Reulen HJ. Fluorescence-guided surgery with 5-aminolevulinic acid for resection of malignant glioma: a randomised controlled multicentre phase III trial. *Lancet Oncol* 2006; **7:** 392–401.

8 Baranski A-C, Schafer M, Bauder-Wüst U, et al. PSMA-11-Derived dual-labeled PSMA inhibitors for preoperative PET imaging and precise fluorescence-guided surgery of prostate cancer. *J Nucl Med* 2018; **59:** 639–45.

9 Wright GL Jr, Haley C, Beckett ML, Schellhammer PF. Expression of prostate-specific membrane antigen in normal, benign, and malignant prostate tissues. *Urol Oncol* 1995; **1:** 18–28.

10 Goodman OB Jr, Barwe SP, Ritter B, et al. Interaction of prostate specific membrane antigen with clathrin and the adaptor protein complex-2. *Int J Oncol* 2007; **31:** 1199–203.

11 Mottet N, van den Bergh RCN, Briers E, et al. EAU-EANM-ESTRO-ESUR-SIOG guidelines on prostate cancer—2020 update. Part 1: screening, diagnosis, and local treatment with curative intent. *Eur Urol* 2021; **79:** 243–62.

12 Sartor O, de Bono J, Chi KN, et al. Lutetium-177-PSMA-617 for metastatic castration-resistant prostate cancer. *N Engl J Med* 2021; **385:** 1091–103.

13 Kularatne SA, Thomas M, Myers CH, et al. Evaluation of novel prostate-specific membrane antigen-targeted near-infrared imaging agent for fluorescence-guided surgery of prostate cancer. *Clin Cancer Res* 2019; **25:** 177–87.

14 Egevad L, Delahunt B, Evans AJ, et al. International Society of Urological Pathology (ISUP) grading of prostate cancer. *Am J Surg Pathol* 2016; **40:** 858–61.

15 Matoso A, Epstein JI. Defining clinically significant prostate cancer on the basis of pathological findings. *Histopathology* 2019; **74:** 135–45.

16 Spizzo G, Fong D, Wurm M, et al. EpCAM expression in primary tumour tissues and metastases: an immunohistochemical analysis. *J Clin Pathol* 2011; **64:** 415–20.

17 Azargoshasb S, Boekestijn I, Roestenberg M, et al. Quantifying the impact of signal-to-background ratios on surgical discrimination of fluorescent lesions. *Mol Imaging Biol* 2023; **1:** 180–89.

18 Kuru TH, Wadhwa K, Chang RT, et al. Definitions of terms, processes and a minimum dataset for transperineal prostate biopsies: a standardization approach of the Ginsburg Study Group for Enhanced Prostate Diagnostics. *BJU Int* 2013; **112:** 568–77.

19 Satish P, Simpson B, Freeman A, et al. Mapping contemporary biopsy zones to traditional prostatic anatomy: the key to understanding relationships between prostate cancer topography, magnetic resonance imaging conspicuity, and clinical risk. *Eur Urol* 2021; **80:** 263–65.

20 Hoogstins CE, Tummers QR, Gaarenstroom KN, et al. A novel tumor-specific agent for intraoperative near-infrared fluorescence imaging: a translational study in healthy volunteers and patients with ovarian cancer. *Clin Cancer Res* 2016; **22:** 2929–38.

21 Boogerd LSF, Hoogstins CES, Schaap DP, et al. Safety and effectiveness of SGM-101, a fluorescent antibody targeting carcinoembryonic antigen, for intraoperative detection of colorectal cancer: a dose-escalation pilot study. *Lancet Gastroenterol Hepatol* 2018; **3:** 181–91.

22 de Valk KS, Deken MM, Handgraaf HJM, et al. First-in-human assessment of cRGD-ZW800-1, a zwitterionic, integrin-targeted, near-infrared fluorescent peptide in colon carcinoma. *Clin Cancer Res* 2020; **26:** 3990–98.

23 Murphy DG, Bjartell A, Ficarra V, et al. Downsides of robot-assisted laparoscopic radical prostatectomy: limitations and complications. *Eur Urol* 2010; **57:** 735–46.

24 Novara G, Ficarra V, Rosen RC, et al. Systematic review and meta-analysis of perioperative outcomes and complications after robot-assisted radical prostatectomy. *Eur Urol* 2012; **62:** 431–52.

25 Cacciamani GE, Maas M, Nassiri N, et al. Impact of pelvic lymph node dissection and its extent on perioperative morbidity in patients undergoing radical prostatectomy for prostate cancer: a comprehensive systematic review and meta-analysis. *Eur Urol Oncol* 2021; **4:** 134–49.

26 Vahrmeijer AL, Hutteman M, van der Vorst JR, van de Velde CJ, Frangioni JV. Image-guided cancer surgery using near-infrared fluorescence. *Nat Rev Clin Oncol* 2013; **10:** 507–18.

27 Silver DA, Pellicer I, Fair WR, Heston WD, Cordon-Cardo C. Prostate-specific membrane antigen expression in normal and malignant human tissues. *Clin Cancer Res* 1997; **3:** 81–85.

28 Pizzuto DA, Müller J, Mühlematter U, et al. The central zone has increased 68Ga-PSMA-11 uptake: "Mickey Mouse ears" can be hot on 68Ga-PSMA-11 PET. *Eur J Nucl Med Mol Imaging* 2018; **45:** 1335–43.

29 Cohen RJ, Shannon BA, Phillips M, Moorin RE, Wheeler TM, Garrett KL. Central zone carcinoma of the prostate gland: a distinct tumor type with poor prognostic features. *J Urol* 2008; **179:** 1762–67.